Non-cell autonomous and spatiotemporal signaling from a tissue organizer orchestrates plant vascular development

BaoJun Yang[1,2,*], Max Minne[1,2], Federica Brunoni[3], Lenka Plačková[3], Ivan Petřík[3], Yanbiao Sun[1,2], Jonah Nolf[1,2], Wouter Smet[1,2], Kevin Verstaen[4,5], Jos R. Wendrich[1,2], Thomas Eekhout[1,2], Klára Hoyerová[6], Gert Van Isterdael[7,8], Jurgen Haustraete[9,10], Anthony Bishopp[11], Etienne Farcot[12], Ondřej Novák[3], Yvan Saeys[4,5] and Bert De Rybel[1,2,*]

[1] Ghent University, Department of Plant Biotechnology and Bioinformatics, Ghent, Belgium
[2] VIB Center for Plant Systems Biology, Ghent, Belgium
[3] Laboratory of Growth Regulators, Institute of Experimental Botany of the Czech Academy of Sciences & Faculty of Science of Palacký University, Šlechtitelů 27, 783 71 Olomouc, Czech Republic
[4] Ghent University, Department of Applied Mathematics, Computer Science and Statistics, Ghent, Belgium
[5] VIB Center for Inflammation Research, Data Mining and Modelling for Biomedicine, Ghent, Belgium
[6] Laboratory of Hormonal Regulations in Plants, Institute of Experimental Botany, Czech Academy of Sciences, Rozvojová 263, 165 02 Prague, Czech Republic
[7] VIB Flow Core, VIB Center for Inflammation Research, Ghent, Belgium
[8] Ghent University, Department of Biomedical Molecular Biology, Ghent, Belgium
[9] VIB Protein Service Facility, VIB Center for Inflammation Research, Ghent, Belgium
[10] Department of Biomedical Molecular Biology, Ghent University, Ghent, Belgium;
[11] University of Nottingham, School of Biosciences, Loughborough, UK
[12] University of Nottingham, School of Mathematical Sciences, Nottingham, UK

*Corresponding authors. Email: bert.derybel@psb.vib-ugent.be and baojun.yang@psb.vib-ugent.be

Abstract:

During plant development, a precise balance of cytokinin is crucial for correct growth and patterning, but it remains unclear how this is achieved across different cell types and in the context of a growing organ. Here we show that, in the root apical meristem, the TMO5/LHW complex increases active cytokinin levels via two cooperatively acting enzymes. By profiling the transcriptomic changes of increased cytokinin at single cell level, we further show that this effect is counteracted by a tissue specific increase in *CYTOKININ OXIDASE 3* expression via direct activation of the mobile transcription factor SHORTROOT. In summary we show that within the root meristem, xylem cells act as a local organizer of vascular development by non-autonomously regulating cytokinin levels in neighboring procambium cells via sequential induction and repression modules.

One-Sentence Summary: Non-cell autonomous and spatiotemporal regulation of cytokinin levels control primary vascular development in Arabidopsis

The plant vasculature is a complex tissue composed of multiple cell types, each with a specific function [1]. In the Arabidopsis root apical meristem during primary growth, vascular tissues are organized according to a bilateral symmetry with a central xylem axis flanked by two phloem poles with intervening procambium cells [1,2]. Previous work has shown that this patterning is established and maintained by a domain of high auxin signaling in the xylem cells and a domain of high cytokinin signaling in the procambium and phloem cell lineages [3-5], making this an excellent model system to study coordinated development involving intercellular communication, hormonal signaling, and crosstalk. On a molecular level, growth and patterning of vascular tissues is in part driven by the heterodimer formed by the basic helix loop helix transcription factors TARGET OF MONOPTEROS 5 and LONESOME HIGHWAY (TMO5/LHW) [6-11]. This complex triggers local biosynthesis of cytokinin via direct activation of LONELY GUY 3 and 4 (LOG3/4) [4,5]. This xylem-derived cytokinin is thought to diffuse to neighboring procambium cells where it drives vascular proliferation by activating downstream target genes, including members of the DNA-binding-with-one-finger (DOF)-type transcription factor family [12,13]. Although it is clear that TMO5/LHW plays an important role in controlling vascular growth and patterning [4,5], it remains unclear how appropriate cytokinin levels are maintained in each cell type in the context of a growing tissue [14].

BGLU44 and LOG4 cooperatively produce active cytokinin downstream of TMO5/LHW

TMO5/LHW activity is dependent on the phytohormone cytokinin as this dimer is inactive when cytokinin biosynthesis (e.g. in a *log1234578* mutant [15,16]) or signaling (e.g. in a *wol* mutant [17]) are perturbed [4]. Although *LOG3* and *LOG4* were identified as main target genes of the TMO5/LHW dimer [4,5], misexpression of *LOG* genes does not result in the strong cytokinin-related vascular phenotypes observed upon exogenous cytokinin treatment or TMO5/LHW induction [4], suggesting that additional factors are involved in releasing active cytokinin. To identify such factors, we overlapped genes co-expressed with *LOG4* in a high spatiotemporal resolution single cell dataset (**Fig. 1a**, **Fig. S1** and **Data S1**) [18] with a list of putative TMO5/LHW target genes [13]. The overlap contained the closely related *LOG3* [4,5], the negative regulator of TMO5/LHW activity *SACL3* [7,11] and an uncharacterized beta-glucosidase family member *BGLU44/AT3G18080* (**Fig. 1a**, **Fig. S2a-c** and **Data S1**). By Q-RT-PCR analysis, we found that relative expression levels of *BGLU44* were increased upon

TMO5/LHW induction and reduced in *tmo5* single, double and triple mutant backgrounds (**Fig. 1b**), similar to *LOG4* [4]. We next constructed a p*BGLU44*-nYFP/GUS reporter line and found *BGLU44* expressed in the root apical meristem along the xylem axis and in xylem pole associated pericycle and endodermis cells as predicted by scRNA-seq atlas data [18] (**Fig. 1c-d**, **Fig. S2a-c**), and identical to *LOG4* expression patterns in this tissue [4]. Induction of the TMO5/LHW heterodimer throughout the root meristem (using a dexamethasone (DEX) double inducible p*RPS5A*::TMO5:GR x p*RPS5A*::LHW:GR or dGR line [13]) triggered both increased and ectopic p*BGLU44*::nYFP/GUS expression (**Fig. 1e-f**, **Fig. S2d-g**), suggesting BGLU44 acts downstream of TMO5/LHW. By ChIP-Q-RT-PCR analysis, we found a significant binding of TMO5-GR/LHW-GR to the *BGLU44* promoter region, indicating *BGLU44* is a direct target of TMO5/LHW (**Fig. S3a**). Taken together, these results confirm the TMO5/LHW-dependent co-expression of *BGLU44* and *LOG4*.

BGLU44 is a member of the glycoside hydrolase family 1, comprising over 40 members in both *Arabidopsis* and rice [19]. Although BGLU proteins have been implicated in various developmental processes including mobilization of storage compounds [20] and reconstruction of cell walls [21], the beta-glucosidase Zm-p60.1 in maize was shown to cleave biologically inactive cytokinin conjugates to release active cytokinin [22]. To investigate the possibility that BGLU44 would have a similar role in Arabidopsis, we misexpressed *BGLU44* from the strong meristematic *RPS5A* promoter [23] (**Fig. S2h-j**) and analyzed xylem differentiation in the root as proxy for active cytokinin levels [4]. As positive control, TMO5/LHW misexpression (dGR line) resulted in a loss of protoxylem differentiation compared to the wild type control situation (**Fig. 1k,l**). We did not observe any differences in the p*RPS5A*::BGLU44 line compared to wild type plants (**Fig. 1g, i, l**, **Fig. S2h**). Considering that the p*RPS5A*::LOG4 misexpression line shows mild vascular defects in the root meristem [4] (**Fig. 1g, h, l**), we hypothesized that both enzymes might work in a cooperative manner. We thus combined both misexpression lines via crossing (p*RPS5A*::LOG4 x p*RPS5A*::BGLU44) and observed a defect in silique positioning on the stem (**Fig. S2h-i**) and an increase in root hairs (**Fig. S2t-w**) as also seen in TMO5/LHW misexpressing [18] and cytokinin overproducing plants [24]. When analyzing the root meristem vascular tissues, we found an almost complete loss of protoxylem differentiation in the root (**Fig. 1j-l**), phenocopying the higher cytokinin levels found in TMO5/LHW misexpression lines [4]. Fitting with this observation, combined misexpression of *LOG4* and *BGLU44* resulted in a small but significant increase in the number of vascular cell files (**Fig. S2k-o**). Similarly, a newly generated *bglu44* loss-of-

function CRISPR line, which led to a large fragment deletion, did not result in a strong phenotype, but enhanced the reduction of vascular cell numbers when combined with *log4* or *log34* mutants (**Fig. S4**). To further corroborate that these phenotypes are related to increased levels of active cytokinin, we next analyzed the TCSn reporter for cytokinin signaling [13,25] fused to the nuclear tdTomato fluorescent protein (pTCSn::ntdT) in the combined misexpression background. Confocal imaging confirmed that plants overexpressing both *LOG4* and *BGLU44*, but not the individual factors, caused increased expression of TCSn, which was most prominent in the ground tissues that typically show very low TCSn expression in wild type plants (**Fig. 1m-q**, **Fig. S2p-s**). Finally, we assayed the enzymatic activity of the BGLU44 protein (for production and purification, see supplemental Materials and Methods). First, we tested specificity of BGLU44 activity *in vitro* for several glucose conjugated CK substrates and found that it is specific to O-glucoside cytokinin species (**Fig. 1r**). Moreover, BGLU44 is able to cleave the inactive conjugated tZOG and tZROG species into the bio-active tZ and tZR (**Fig. 1s** and **Data S5**). Measuring the endogenous cytokinin profiles of 7-day-old root tips in LOG4, BGLU44, LOG4/BGLU44 and dGR misexpression lines revealed that the combined misexpression of LOG4 and BGLU44 resulted in a similar increase in cytokinin levels as previously shown for TMO5/LHW [4] (**Fig. 1t** and **Data S5**). Taken together, our results show that BGLU44 and LOG4 cooperatively act downstream of TMO5/LHW to release active cytokinin in the vascular bundle of the root meristem, hereby controlling primary vascular development.

CKX3 balances cytokinin levels downstream of TMO5/LHW

Cytokinin levels need to be well balanced in space and time to allow normal development. Indeed, high levels of active cytokinin disturb normal vascular cell proliferation, patterning and differentiation [15,16,26,27] (**Fig. 3n**). The active cytokinin produced in the central xylem axis - where TMO5/LHW activity overlaps with *LOG4* and *BGLU44* expression - is thought to diffuse to neighboring procambium and phloem cells [3-5] which show high levels of cytokinin signaling. In order to understand the tissue specific responses of increased cytokinin levels, we profiled the transcriptional effect of cytokinin treatment on root meristem cells at single cell resolution (**Fig. 2a-b**) (see Supplemental Materials and Methods section for experimental details and analysis pipeline). After filtering, we retained about 10K high quality cells for each sample with a minimal UMI count of more than 1000 (**Fig. 2a**). Clear transcriptional changes are observed for most cell types, while some subpopulations remain largely

unaffected such as e.g. the protoxylem and columella cells (**Fig. S5a-c**), suggesting tissue-specific responses. As expected, primary response genes of the cytokinin signaling pathway such as A-type *ARABIDOPSIS RESPONSE REGULATORS* (*ARR*) were recovered as cytokinin inducible in all cell clusters (**Data S2**). We next created transcriptional reporter lines for 12 genes previously uncharacterized for cytokinin response in the root meristem and showing tissue specific cytokinin responses. These lines show both the predicted tissue specific expression pattern in the mock situation and the tissue specific induction kinetics after cytokinin treatment in the root (**Fig. S6**), thus validating the predictive power of our dataset.

Given that procambium cells are those responding to cytokinin levels with respect to cell proliferation in our system, we next searched our dataset for those genes specifically responding to the increase in cytokinin levels in the procambium cell cluster only. We found that among the top candidates, *CYTOKININ OXIDASE3* (*CKX3/AT5G56970*) was recovered as specifically induced by cytokinin in procambium cells (**Fig. 2c-d** and **Data S3**). As CKX proteins have been shown to reduce levels of active cytokinin [26,28], CKX3 could be the factor to counteract the flow of active cytokinin from the xylem cells and ensure well balanced cytokinin levels. Indeed, previous reports suggested that cytokinin could balance itself by promoting cytokinin oxidase expression [29,30]. We confirmed the cytokinin inducibility *CKX3* in procambium cells by generating a p*CKX3*::nYFP-GUS transcriptional reporter using a 4.2kb promoter fragment (**Fig. 2e-f**). Upon transfer to 10 µM BAP for 3h, a significant increase in *CKX3* expression levels in procambium cells was observed (**Fig. 2g-i**) as predicted by the scRNA-seq dataset (**Fig. 2c-d** and **Fig. S5e**).

To further understand if the *CKX3* regulation by cytokinin is related to TMO5/LHW, we first confirmed by Q-RT-PCR that relative expression levels are increased upon induction of the TMO5/LHW heterodimer and downregulated in *tmo5* double and triple mutants (**Fig. 3a**), supporting that CKX3 indeed acts downstream of TMO5/LHW. We next introduced the transcriptional p*CKX3*::nYFP/GUS line (**Fig. 3b-e**) and a newly generated translational p*CKX3*::CKX3:GFP reporter lines (**Fig. 3f-i**) in the dGR background. Upon misexpression of TMO5/LHW, expression of *CKX3* increased and now marked the entire vascular cylinder (**Fig. 3d-e**, **h-i**). To further assess a possible role for CKX3 during vascular development, we analyzed phenotypes upon loss of function of CKX3 and its close homolog CKX5, which shows a similar expression pattern as predicted by our scRNA-seq dataset (**Fig. S5f**, **S7a-b**) and validated by a newly generated 3.5kb p*CKX5*::nYFP/GUS reporter line (**Fig. S7c-d**). The

ckx3 ckx5 double mutant [24], but not the *ckx3* or *ckx5* single mutants, showed additional metaxylem cell files in over 60% of plants analyzed (**Fig. S7e-h, l**) and vascular cell file number was increased (**Fig. S7m-q**). This is opposite to the effect of reducing cytokinin biosynthesis in *log* higher order mutants (**Fig. S7i-l**) [4,16]. These results suggest that CKX3 (in collaboration with CKX5) is involved in modulating vascular cytokinin levels. To further investigate the importance of CKX3 function downstream of TMO5/LHW, we generated p*RPS5A*::CKX3:YFP misexpression lines in the dGR background. Unlike the dGR control situation where DEX treatment inhibited protoxylem differentiation (**Fig. 3j-k, o**) and increased vascular cell file number (**Fig. 3p-q, t**) [6], CKX3 misexpression completely repressed TMO5/LHW function (**Fig. 3l-m, o, r-t**). These results show that TMO5/LHW not only promotes release of active cytokinin via LOG4 and BGLU44, but at the same time represses active cytokinin in procambium cells via CKX3 in order to maintain optimal levels of cytokinin for normal vascular development. To further examine the importance of TMO5/LHW in CKX3 regulation, we treated wild type and *tmo5* triple mutants with exogenous cytokinin. While cytokinin increased relative expression levels of *CKX3* in a wild type Col-0 background, this response was repressed in the absence of TMO5 activity (**Fig. S7r**) suggesting that TMO5/LHW is an important regulator of *CKX3* expression. Considering *TMO5* and *CKX3* expression domains are in neighboring cell types, we hypothesize there must be a mobile intermediate connecting these two factors.

SHR bridges TMO5/LHW-dependent regulation of *CKX3* expression

The mobile transcription factor SHORT-ROOT (SHR) has been shown to directly bind to the *CKX3* promoter region and regulate its expression levels [31]. Although cytokinin levels [31] and signaling (**Fig. S8a-c**) are high in a *shr-2* mutant background, *CKX3* expression levels are reduced [31]. This suggests that although *CKX3* expression levels can be controlled by cytokinin and SHR, both mobile in the vascular tissues, the dominant form of regulation acts via SHR. To explore the importance of SHR in the connection between TMO5/LHW and CKX3 regulation during vascular development, we first introduced a p*SHR*::SHR:GFP translational reporter line in dGR plants. Upon induction of TMO5/LHW by DEX treatment, the SHR:GFP fusion protein was ectopically present throughout the root meristem (**Fig. S8d-g**). To understand if this was caused by regulation at the transcriptional level, we next introduced a p*SHR*::nYFP/GUS transcriptional reporter line in dGR. Also in this case, induction of TMO5/LHW caused ectopic expression of *SHR* throughout the root meristem

(**Fig. 4a-d**), suggesting TMO5/LHW might control *SHR* expression. These results were further supported by Q-RT-PCR data showing relative expression levels of *SHR* were increased in a TMO5/LHW heterodimer misexpression line and repressed in *tmo5* higher order mutant lines (**Fig. S8h**). To evaluate if TMO5/LHW directly activates *SHR* expression, we fused a 2.5kb promoter fragment of *SHR* [32] to luciferase and introduced this construct in tobacco leaves in the presence of TMO5/LHW. p*SHR*::LUC was induced by TMO5/LHW, while this was not the case in the negative controls and not significantly different in presence of the individual members of the dimer (**Fig. 4e-f**), fitting with the previous findings that TMO5 and LHW act as obligate heterodimer [6,9]. These results were confirmed by ChIP-Q-RT-PCR (**Fig. S3b**). Taken together, these results suggest that TMO5/LHW directly binds to the *SHR* promoter region to activate its expression.

To further study the genetic relationship between SHR and the TMO5/LHW heterodimer complex, we introduced the *shr-2* mutation [33] into a dGR background by crossing. Although some periclinal divisions were still observed, vascular cell file numbers were not significantly increased in the presence of the *shr-2* mutation (**Fig. 4g-k**), suggesting that SHR is required for normal TMO5/LHW function. We observed a loss of protoxylem differentiation in *shr-2* both with and without induction of dGR (**Fig. S8i-m**), in line with the high cytokinin levels in this mutant background [31]. Moreover, we found that xylem expressed SHR (p*TMO5*::SHR:GFP) is capable of moving throughout the vascular bundle (**Fig. 4l-o**), and is capable of rescuing the *shr-2* root length and ground tissue cell identity phenotypes in a dose-dependent manner (**Fig. S9**). This indicates that TMO5/LHW driven SHR protein can move from xylem cells into adjacent procambium cells to regulate *CKX3* expression and in this way balance overall cytokinin levels. The relevance of TMO5/LHW regulation on the extended SHR transcriptional pathway was further highlighted by the fact that also its interactor SCARECROW and downstream target miRNA165 are controlled by TMO5/LHW activity (**Fig. S8n-s**). As such, the xylem axis work as a central organizer for vascular development and patterning via SHR.

Spatiotemporal regulation of cytokinin levels during vascular development

Our results suggest that downstream of TMO5/LHW, the LOG4 and BGLU44 enzymes cooperatively work to increase levels of active cytokinin in the xylem axis, while CKX3 reduces cytokinin levels in the neighboring procambium cells via SHR as mobile

intermediate, and independent of cytokinin signaling. These results are in line with the hypothesis that the xylem axis acts as an insensitive source of active cytokinin which is thought to diffuse to the neighboring procambium cells [4,5]. In the procambium domain, cells are responsive to cytokinin [3,4,17,27] and thus require a repressive mechanism to cope with the influx of active cytokinin and obtain optimal levels for normal development. We next questioned if these different factors responsible for the increase and decrease of active cytokinin levels are activated simultaneously or in sequence. By analyzing the temporal changes in expression levels via Q-RT-PCR, we show that *LOG4* is increased in expression levels around 30'-1h after TMO5/LHW induction (**Fig. 4p**), quickly followed by *BGLU44* induction starting around 1h after induction (**Fig. 4q**). *SHR* expression levels are also induced from 1h onwards (**Fig. 4r**), leading to the induction of *CKX3* as direct SHR target at 3h after induction (**Fig. 4s**). A similar trend was observed when analyzing the transcriptional reporter lines for *LOG4*, *BGLU44* and *SHR*, and a protein fusion reporter for *CKX3* genes (**Fig. S10a-c**, **Fig. S11**), further corroborating that induction of active cytokinin levels via LOG4 and BGLU44, and repression via SHR and CKX3 are sequential events upon TMO5/LHW induction. In order to better understand the spatiotemporal wiring of this network, we generated a mathematical model comprising these molecular players in their respective cells (for a detailed description, see **Supplemental Materials and Methods**) with auxin signaling as input to TMO5/LHW and cytokinin signaling as output. In this model, the wiring of activation and repression modules is capable of dampening fast oscillating auxin inputs into a continuous cytokinin response, while remaining responsive to slower changes of auxin (see Model Description). This response was not dependent on the amplitude of the auxin signaling input, meaning that both small and large changes have an impact on the cytokinin signaling output as long as the frequency of the modulation is low (see Model Description).

In conclusion, our findings point to a tight spatiotemporal regulation of cytokinin levels via sequential induction and repression modules, all originating from the same bHLH heterodimer complex (**Fig. S12**). As such, we found that a single transcription factor complex controls multiple biosynthesis and degradation steps of a phytohormone to regulate tissue development in space and time. The fact that these modules with opposite function are initiated as direct targets of the TMO5/LHW complex, suggests that cytokinin levels might be balanced without the need for intermediate sensing via canonical CRE1/AHK4/WOL receptor signaling [17,34]. Rather, differences in spatiotemporal activity of these modules might

be sufficient to control levels of active cytokinin in the respective tissues and drive the observed self-organizing capacities of vascular patterning and growth [4,35,36]. Intriguingly, our modeling efforts suggest that these cytokinin signaling controlled processes would not be influenced by fast fluctuations in auxin signaling in the root apical meristem. Rather, vascular patterning and growth controlled by the TMO5/LHW dimer would be sensitive to slow and gradual changes in the auxin input. Although additional experimental work is required to support this hypothesis, this emerging property of the model makes sense in the context of a growing tissue where growth and patterning responds to gradual modulation of hormone levels. Our work also identifies the central xylem cells as a tissue organizer for vascular development and highlights TMO5/LHW as upstream regulator of SHR, a central transcriptional hub controlling several distinct aspects of growth and development in vascular and other tissues [33,40-42].Given that MP was previously shown to control SHR expression [43], it is conceivable that within the context of vascular development this regulation is indirect, and requires TMO5 as an intermediate factor. It remains to be determined if and how TMO5/LHW would be connected to other SHR-controlled processes during plant development.

References

1 Lucas, W. J. *et al.* The plant vascular system: evolution, development and functions. *J Integr Plant Biol* **55**, 294-388, doi:10.1111/jipb.12041 (2013).

2 De Rybel, B., Mahonen, A. P., Helariutta, Y. & Weijers, D. Plant vascular development: from early specification to differentiation. *Nature reviews. Molecular cell biology* **17**, 30-40, doi:10.1038/nrm.2015.6 (2016).

3 Bishopp, A. *et al.* A mutually inhibitory interaction between auxin and cytokinin specifies vascular pattern in roots. *Current biology* **21**, 917-926, doi:10.1016/j.cub.2011.04.017 (2011).

4 De Rybel, B. *et al.* Plant development. Integration of growth and patterning during vascular tissue formation in Arabidopsis. *Science* **345**, 1255215, doi:10.1126/science.1255215 (2014).

5 Ohashi-Ito, K. *et al.* A bHLH complex activates vascular cell division via cytokinin action in root apical meristem. *Curr Biol* **24**, 2053-2058, doi:10.1016/j.cub.2014.07.050 (2014).

6 De Rybel, B. *et al.* A bHLH complex controls embryonic vascular tissue establishment and indeterminate growth in Arabidopsis. *Developmental cell* **24**, 426-437, doi:10.1016/j.devcel.2012.12.013 (2013).

7 Katayama, H. *et al.* A Negative Feedback Loop Controlling bHLH Complexes Is Involved in Vascular Cell Division and Differentiation in the Root Apical Meristem. *Curr Biol* **25**, 3144-3150, doi:10.1016/j.cub.2015.10.051 (2015).

8 Ohashi-Ito, K. & Bergmann, D. C. Regulation of the Arabidopsis root vascular initial population by LONESOME HIGHWAY. *Development (Cambridge, England)* **134**, 2959-2968, doi:10.1242/dev.006296 (2007).

9 Ohashi-Ito, K., Matsukawa, M. & Fukuda, H. An atypical bHLH transcription factor regulates early xylem development downstream of auxin. *Plant Cell Physiol* **54**, 398-405, doi:10.1093/pcp/pct013 (2013).

10 Ohashi-Ito, K., Oguchi, M., Kojima, M., Sakakibara, H. & Fukuda, H. Auxin-associated initiation of vascular cell differentiation by LONESOME HIGHWAY. *Development* **140**, 765-769, doi:10.1242/dev.087924 (2013).

11 Vera-Sirera, F. *et al.* A bHLH-Based Feedback Loop Restricts Vascular Cell Proliferation in Plants. *Dev Cell* **35**, 432-443, doi:10.1016/j.devcel.2015.10.022 (2015).

12 Miyashima, S. *et al.* Mobile PEAR transcription factors integrate positional cues to prime cambial growth. *Nature* **565**, 490-494, doi:10.1038/s41586-018-0839-y (2019).
13 Smet, W. *et al.* DOF2.1 Controls Cytokinin-Dependent Vascular Cell Proliferation Downstream of TMO5/LHW. *Current biology : CB* **29**, 520-529 e526, doi:10.1016/j.cub.2018.12.041 (2019).
14 Wybouw, B. & De Rybel, B. Cytokinin - A Developing Story. *Trends in plant science* **24**, 177-185, doi:10.1016/j.tplants.2018.10.012 (2019).
15 Kuroha, T. *et al.* Functional analyses of LONELY GUY cytokinin-activating enzymes reveal the importance of the direct activation pathway in Arabidopsis. *The Plant Cell* **21**, 3152-3169, doi:10.1105/tpc.109.068676 (2009).
16 Tokunaga, H. *et al.* Arabidopsis lonely guy (LOG) multiple mutants reveal a central role of the LOG-dependent pathway in cytokinin activation. *The Plant journal* **69**, 355-365, doi:10.1111/j.1365-313X.2011.04795.x (2012).
17 Mähönen, A. P. *et al.* A novel two-component hybrid molecule regulates vascular morphogenesis of the Arabidopsis root. *Genes & development* **14**, 2938-2943 (2000).
18 Wendrich, J. R. *et al.* Vascular transcription factors guide plant epidermal responses to limiting phosphate conditions. *Science* **370**, doi:10.1126/science.aay4970 (2020).
19 Xu, Z. *et al.* Functional genomic analysis of Arabidopsis thaliana glycoside hydrolase family 1. *Plant Mol Biol* **55**, 343-367, doi:10.1007/s11103-004-0790-1 (2004).
20 Leah, R., Kigel, J., Svendsen, I. & Mundy, J. Biochemical and molecular characterization of a barley seed beta-glucosidase. *J Biol Chem* **270**, 15789-15797, doi:10.1074/jbc.270.26.15789 (1995).
21 Dharmawardhana, D. P., Ellis, B. E. & Carlson, J. E. A beta-glucosidase from lodgepole pine xylem specific for the lignin precursor coniferin. *Plant Physiol* **107**, 331-339, doi:10.1104/pp.107.2.331 (1995).
22 Brzobohatý, B. *et al.* Release of active cytokinin by a beta-glucosidase localized to the maize root meristem. *Science* **262**, 1051-1054, doi:10.1126/science.8235622 (1993).
23 Weijers, D. *et al.* An Arabidopsis Minute-like phenotype caused by a semi-dominant mutation in a RIBOSOMAL PROTEIN S5 gene. *Development* **128**, 4289-4299 (2001).
24 Bartrina, I., Otto, E., Strnad, M., Werner, T. & Schmülling, T. Cytokinin regulates the activity of reproductive meristems, flower organ size, ovule formation, and thus seed

356 yield in Arabidopsis thaliana. *Plant Cell* **23**, 69-80, doi:10.1105/tpc.110.079079
357 (2011).
358 25 Zurcher, E. *et al.* A robust and sensitive synthetic sensor to monitor the transcriptional
359 output of the cytokinin signaling network in planta. *Plant Physiology* **161**, 1066-1075,
360 doi:10.1104/pp.112.211763 (2013).
361 26 Werner, T., Motyka, V., Strnad, M. & Schmülling, T. Regulation of plant growth by
362 cytokinin. *Proc Natl Acad Sci U S A* **98**, 10487-10492, doi:10.1073/pnas.171304098
363 (2001).
364 27 Matsumoto-Kitano, M. *et al.* Cytokinins are central regulators of cambial activity.
365 *Proceedings of the National Academy of Sciences of the United States of America*
366 **105**, 20027-20031, doi:10.1073/pnas.0805619105 (2008).
367 28 Schmülling, T., Werner, T., Riefler, M., Krupková, E. & Bartrina y Manns, I.
368 Structure and function of cytokinin oxidase/dehydrogenase genes of maize, rice,
369 Arabidopsis and other species. *J Plant Res* **116**, 241-252, doi:10.1007/s10265-003-
370 0096-4 (2003).
371 29 Lee, D. J. *et al.* Genome-wide expression profiling of ARABIDOPSIS RESPONSE
372 REGULATOR 7(ARR7) overexpression in cytokinin response. *Mol Genet Genomics*
373 **277**, 115-137, doi:10.1007/s00438-006-0177-x (2007).
374 30 Rashotte, A. M., Carson, S. D., To, J. P. & Kieber, J. J. Expression profiling of
375 cytokinin action in Arabidopsis. *Plant Physiol* **132**, 1998-2011,
376 doi:10.1104/pp.103.021436 (2003).
377 31 Cui, H. *et al.* Genome-wide direct target analysis reveals a role for SHORT-ROOT in
378 root vascular patterning through cytokinin homeostasis. *Plant Physiol* **157**, 1221-
379 1231, doi:10.1104/pp.111.183178 (2011).
380 32 Marquès-Bueno, M. D. M. *et al.* A versatile Multisite Gateway-compatible promoter
381 and transgenic line collection for cell type-specific functional genomics in
382 Arabidopsis. *Plant J* **85**, 320-333, doi:10.1111/tpj.13099 (2016).
383 33 Levesque, M. P. *et al.* Whole-genome analysis of the SHORT-ROOT developmental
384 pathway in Arabidopsis. *PLoS biology* **4**, e143 (2006).
385 34 Mähönen, A. P. *et al.* Cytokinin signaling and its inhibitor AHP6 regulate cell fate
386 during vascular development. *Science (New York, N.Y* **311**, 94-98,
387 doi:10.1126/science.1118875 (2006).

35 Help, H., Mahonen, A. P., Helariutta, Y. & Bishopp, A. Bisymmetry in the embryonic root is dependent on cotyledon number and position. *Plant signaling & behavior* **6**, 1837-1840, doi:10.4161/psb.6.11.17600 (2011).

36 Mellor, N. *et al.* Theoretical approaches to understanding root vascular patterning: a consensus between recent models. *Journal of experimental botany* **68**, 5-16, doi:10.1093/jxb/erw410 (2017).

37 De Smet, I. *et al.* Auxin-dependent regulation of lateral root positioning in the basal meristem of Arabidopsis. *Development* **134**, 681-690 (2007).

38 De Rybel, B. *et al.* A novel Aux/IAA28 signaling cascade activates GATA23-dependent specification of lateral root founder cell identity. *Current biology* **20**, 1697-1706, doi:10.1016/j.cub.2010.09.007 (2010).

39 Moreno-Risueno, M. A. *et al.* Oscillating gene expression determines competence for periodic Arabidopsis root branching. *Science* **329**, 1306-1311, doi:10.1126/science.1191937 (2010).

40 Helariutta, Y. *et al.* The SHORT-ROOT gene controls radial patterning of the Arabidopsis root through radial signaling. *Cell* **101**, 555-567 (2000).

41 Nakajima, K., Sena, G., Nawy, T. & Benfey, P. N. Intercellular movement of the putative transcription factor SHR in root patterning. *Nature* **413**, 307-311 (2001).

42 Sozzani, R. *et al.* Spatiotemporal regulation of cell-cycle genes by SHORTROOT links patterning and growth. *Nature* **466**, 128-132, doi:10.1038/nature09143 (2010).

43 Möller, B. K. *et al.* Auxin response cell-autonomously controls ground tissue initiation in the early. *Proc Natl Acad Sci U S A* **114**, E2533-E2539, doi:10.1073/pnas.1616493114 (2017).

Acknowledgments:

The authors thank Dolf Weijers for sharing unpublished materials, Thomas Schmülling for sharing *ckx3*, ckx5, *ckx3 ckx5* seeds and Karin Ljung for stimulating discussions. This work was funded by The Research Foundation - Flanders (FWO; Odysseus II G0D0515N and post-doc fellowship 1215820N); the Netherlands Organization for Scientific Research (NWO; VIDI 864.13.00); Ghent University (BOF20/GOA/012 and BOF18/PDO/151); the European Research Council (ERC Starting Grant TORPEDO; 714055); the China Scholarship Council (file number 202009350010); the Ministry of Education, Youth and Sports of the Czech Republic (European Regional Development Fund-Project "Plants as a tool for sustainable global development" No. CZ.02.1.01/0.0/0.0/16_019/ 0000827), and the Internal Grant Agency of Palacký University (IGA_PrF_2021_011).

Author contributions:

B.D.R. and B. Y. conceived the project and designed experiments; F.B., L.P., I.P., K.H. and O.N. performed enzymatic assays and cytokinin measurements; J.N. produced and purified BGLU44 protein with the help of J.H.; M.M., K.V., T.E. and Y.S. analyzed single cell data; E.F. and A.B. performed the mathematical modeling; B.Y., M.M., Y.S., W.S. and J.R.W performed all other experiments; B.D.R. supervised the project; B.Y. and B.D.R. wrote the paper with input from all authors.

Competing interests:

Authors declare that they have no competing interests.

Data availability:

Upon acceptance, the scRNA-seq data will be made accessible via an on-line browser tool (http://bioit3.irc.ugent.be/plant-sc-atlas/) and raw data can be accessed at NCBI with GEO number: GSE179820. All other data are either in the main paper or the Supplement. Material requests should be directed to the corresponding authors.

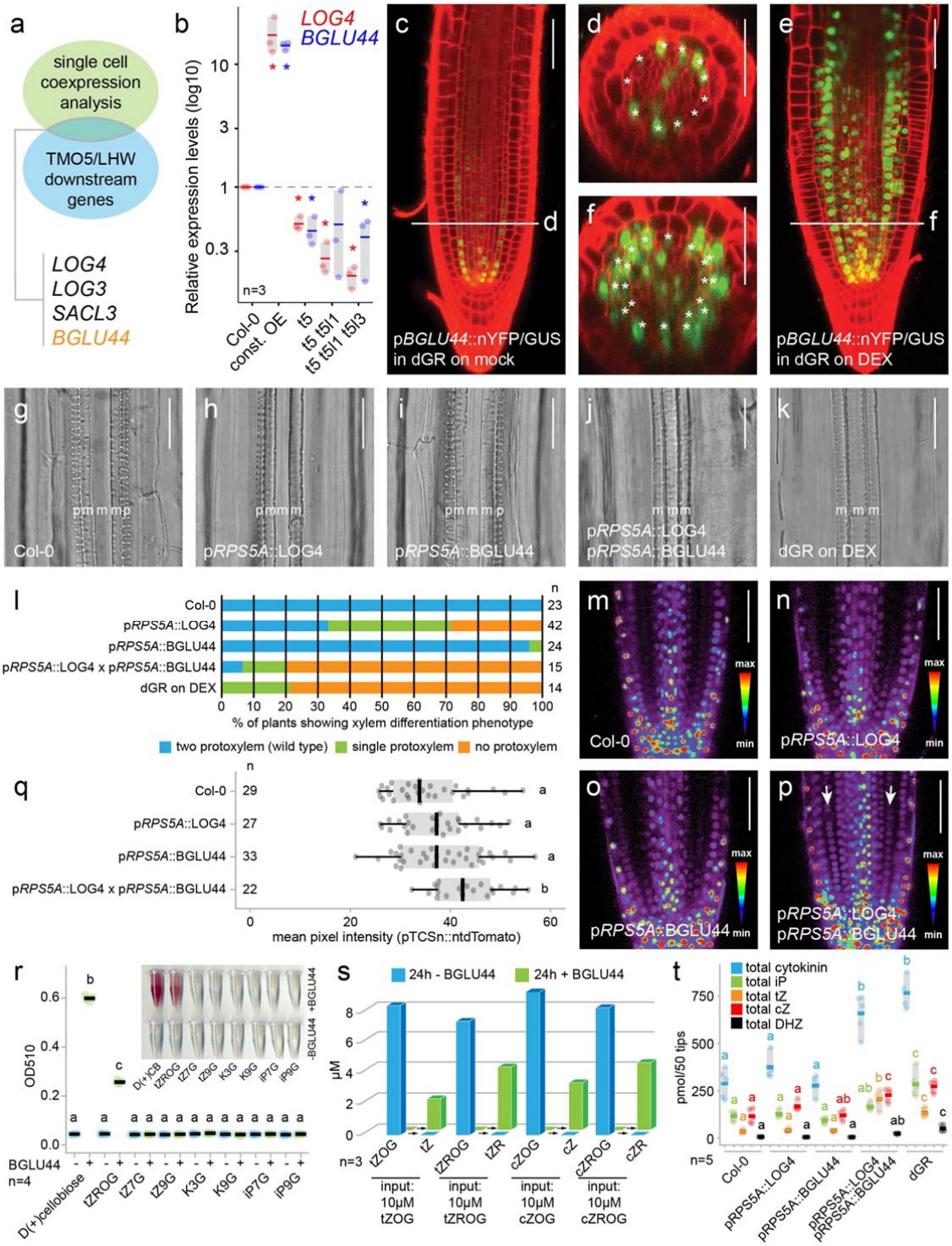

Fig. 1. BGLU44 and LOG4 cooperatively produce active cytokinin downstream of TMO5/LHW. a, Schematic representation of the strategy to identify *BGLU44* as putative target gene of TMO5/LHW. **b**, Relative expression levels of *BGLU44* and *LOG4* in wild type (Col-0), TMO5/LHW misexpression, and *tmo5, tmo5 tmo5like1* (*t5 t5l1*) and *tmo5 tmo5like1 tmo5like3* (*t5 t5l1 t5l3*) mutant backgrounds. **c-f**, Expression of p*BGLU44*::nYFP/GUS in the

dGR root meristem grown on mock medium and transferred to mock or 10 μM DEX for 24h. Asterisks indicate endodermis cell layer. **g-k**, Microscopic images of xylem differentiation in the mentioned genotypes. p: protoxylem, m: metaxylem. **l**, Quantification of the different classes of xylem phenotypes shown in panels g-k. **m-p**, Confocal images of root meristems expressing pTCSn::ntdTomato reporter in the mentioned genotypes. Arrows in p indicate cortex cell layer. **q**, Quantification of the pTCSn::ntdTomato mean pixel intensity in the mentioned genotypes. **r**, *in vitro* BGLU44 enzymatic activity on a range of cytokinin glycoside substrates. **s**, *in vitro* cleavage of O-glucosylated cytokinins by BGLU44. **t**, Overview of total endogenous cytokinin levels in root tips of the indicated lines. Lower-case letters in graphs indicate significantly different groups as determined by one-way ANOVA with post-hoc Tukey HSD testing ($p<0.001$). Asterisks in graphs indicate significance values as determined by standard two-sided t-tests. Black lines indicates mean values and grey boxes indicate data ranges. Scale bars in c-k and m-p are 50 μm. In all panels, n represents the number of replicates or data points.

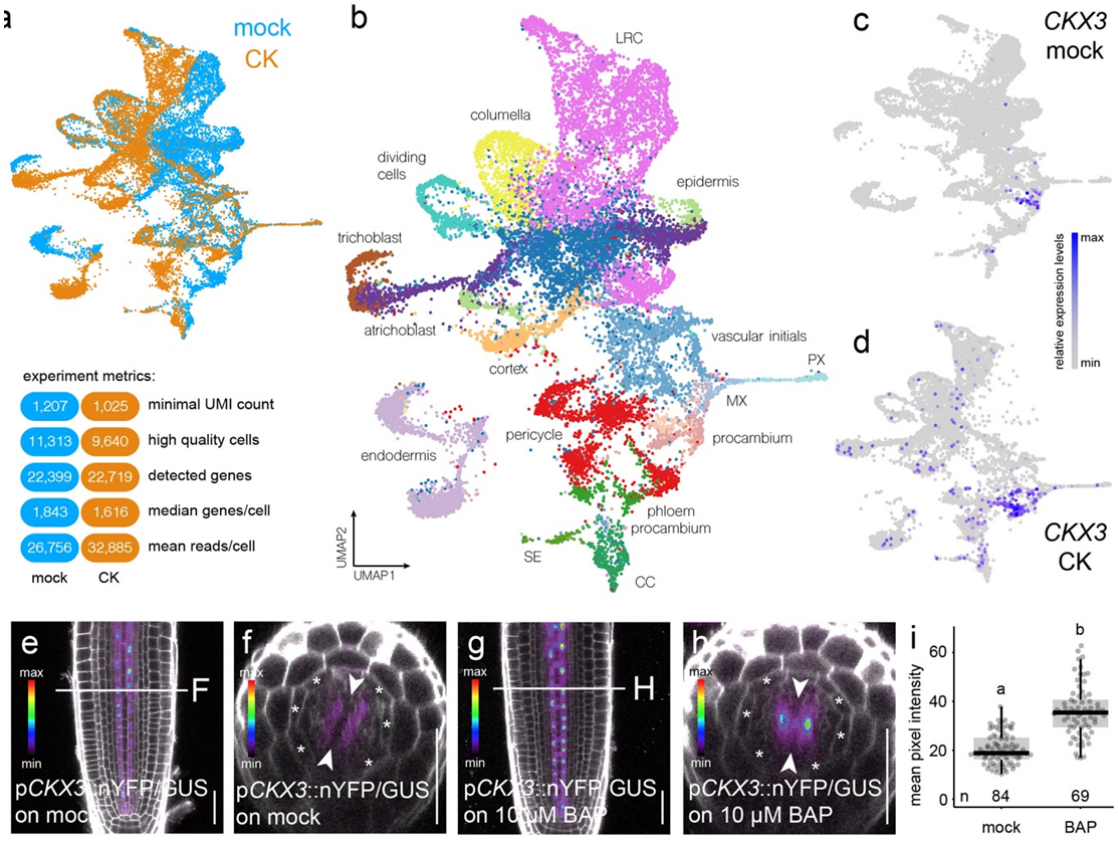

Fig. 2 Single cell transcriptional changes in root meristem cells upon cytokinin treatment. a, UMAP plot showing the merge of the mock and CK samples and an overview of the experimental metrics for both samples. **b**, UMAP plot of the merged data with indications of the different cell identities. LRC: lateral root cap; PX: protoxylem; MX: metaxylem; SE: sieve element; CC: companion cell. The most central dark blue cell cluster is the initial cell cluster. **c-d**, feature plots of *CKX3* expression in the mock (c) and CK (d) datasets showing a tissues specific induction in the procambium cells. **e-h**, Expression of p*CKX3*::nYFP/GUS in the root meristem grown on mock medium and transferred to mock or 10 µM BAP for 3h. Asterisks indicate endodermis cell layer. Arrowheads indicate xylem axis. Scale bars are 50 µm. **i**, Quantification of the experiment described in E-H. Lower-case letters on top of the boxplots indicate significantly different groups as determined by one-way ANOVA with post-hoc Tukey HSD testing ($p<0.001$). In all panels, n represents the number of replicates or data points.

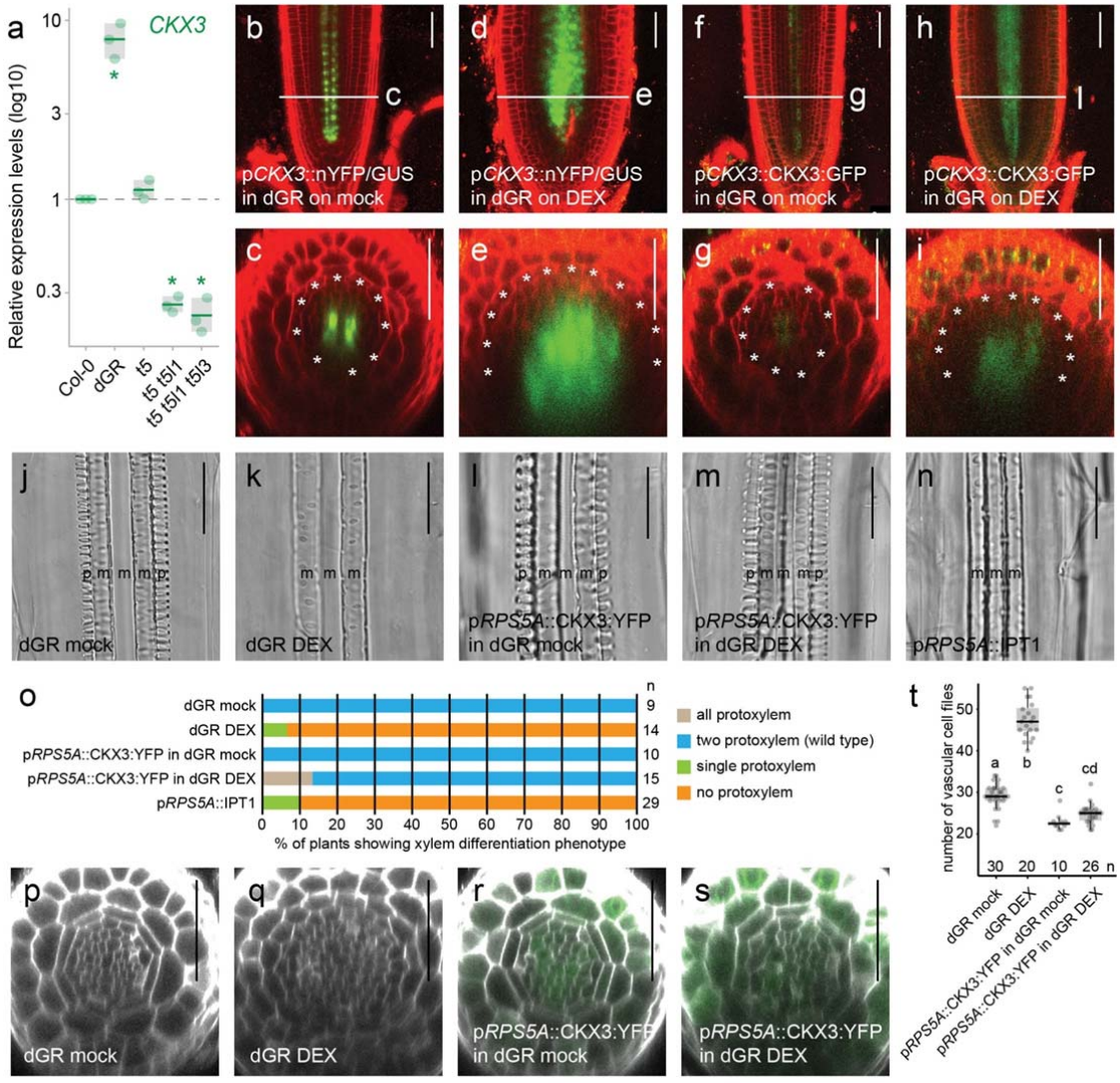

Fig. 3 CKX3 balances cytokinin levels downstream of TMO5/LHW a, Relative expression levels of *CKX3* in wild type (Col-0), TMO5/LHW misexpression, and *tmo5*, *tmo5 tmo5like1* (*t5 t5l1*) and *tmo5 tmo5like1 tmo5like3* (*t5 t5l1 t5l3*) mutant backgrounds. **b-i**, Expression of p*CKX3*::nYFP/GUS and p*CKX3*::CKX3:GFP in the dGR root meristem grown on mock medium and transferred to mock or 10 µM DEX for 24h. Asterisks indicate endodermis cell layer. **j-n**, Microscopic images of xylem differentiation in the mentioned genotypes. p: protoxylem, m: metaxylem. **o**, Quantification of the different classes of xylem phenotypes shown in panels j-n. **p-s**, Confocal cross section images through the root meristem of the mentioned genotypes grown on mock medium and transferred to mock or 10 µM DEX for 24h. **t**, Quantification of the number of vascular cell files shown in panels p-s. Lower-case letters on top of the boxplots indicate significantly different groups as determined by one-way ANOVA with post-hoc Tukey HSD testing ($p<0.001$). Asterisks in graphs

484 indicate significance values as determined by standard two-sided t-tests. Black lines indicates
485 mean values and grey boxes indicate data ranges. Scale bars in b-n and p-s are 50 μm. In all
486 panels, n represents the number of replicates or data points.

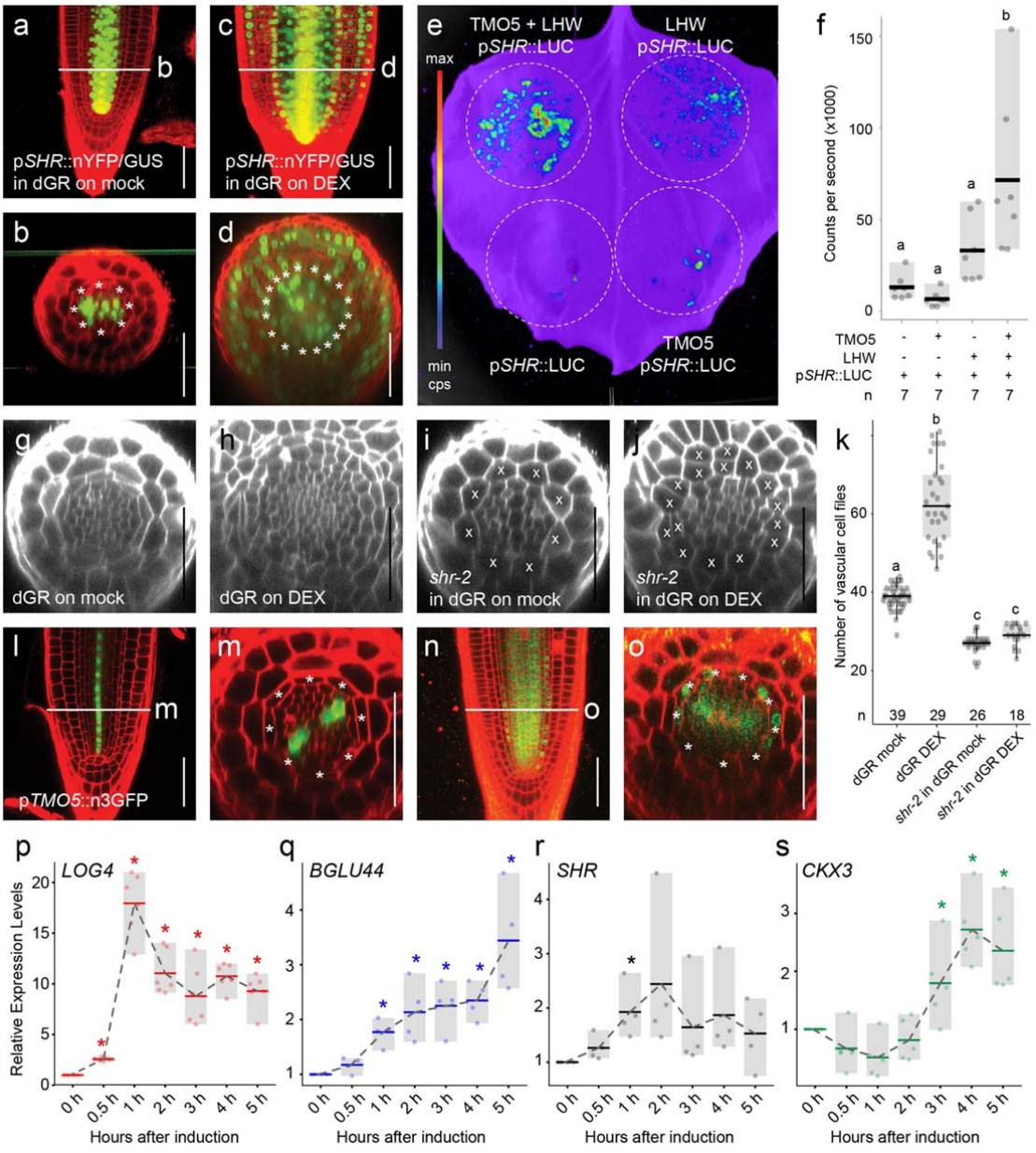

487

488 **Fig. 4 SHR bridges TMO5/LHW-dependent regulation of *CKX3* expression. a-d**,
489 Expression of p*SHR*::nYFP/GUS in the dGR root meristem grown on mock medium and
490 transferred to mock or 10 µM DEX for 24h. Asterisks indicate endodermis cell layer. **e-f**,
491 Transient Luciferase assay in Tobacco leaves showing p*SHR*::LUC expression in the
492 mentioned combination of introduced constructs. **g-j**, Confocal cross section images through
493 the root meristem of the mentioned genotypes grown on mock medium and transferred to
494 mock or 10 µM DEX for 24h. **k**, Quantification of the number of vascular and endodermis
495 cell files shown in panels g-j. The x in panels i and j indicate cells with mixed cortex-
496 endodermis identity in the *shr-2* mutant. **l-o**, Expression of p*TMO5*::n3GFP and

p*TMO5*::SHR:GFP in the root meristem grown on mock medium. **p-s**, Relative expression levels of *LOG4*, *BGLU44*, *SHR* and *CKX3* in dGR grown on mock and transferred to 10 μM DEX for the indicated time before sampling. Lower-case letters on top of the graphs indicate significantly different groups as determined by one-way ANOVA with post-hoc Tukey HSD testing ($p<0.001$). Asterisks in graphs indicate significance values as determined by standard two-sided t-tests. Black lines indicates mean values and grey boxes indicate data ranges. In all panels, n represents the number of replicates or data points.